A FLOW-THROUGH HIGH-PRESSURE ELECTRICAL CONDUCTANCE CELL FOR DETERMINATION OF ION ASSOCIATION OF AQUEOUS ELECTROLYTE SOLUTIONS AT HIGH TEMPERATURE AND PRESSURE

Patience C. Ho[a], Donald A. Palmer[a], Hugo Bianchi[b], and Robert H. Wood[c]
[a] Oak Ridge National Laboratory, P. O. Box 2008, Oak Ridge, TN 37831-6110, USA,
[b] Comision Nacional de Energia Atomica, Buenos Aires, Argentina,
[c] University of Delaware, Newark, Delaware 19716, USA

ABSTRACT

A flow-through high-pressure electrical conductance cell was designed and constructed to measure limiting molar conductances and ion association constants of dilute aqueous solutions with high precision at high temperatures and pressures. The basic concept of the cell employs the principle developed at the University of Delaware in 1995, but overall targets higher temperatures (to 600°C) and pressures (to 300 MPa). At present the cell has been tested by measuring aqueous NaCl and LiOH solutions (10^{-3} to 10^{-5} mol·kg^{-1}) to 405°C and 33 MPa with good results.

INTRODUCTION

In aqueous solutions all electrolytes tend to associate at high temperatures and low solution densities. Knowledge of the association constants is important in interpreting the thermodynamics of ion-ion and ion-water interactions in solutions from sub- to super-critical conditions where the thermodynamic properties of electrolytes undergo dramatic changes. Conductance data not only provide a basic understanding of the behavior of electrolytes under extreme conditions, but also yield information relevant to geochemical systems, the chemistry occurring in water/steam cycles in power plants, nuclear waste disposal, and supercritical water degradation of organic wastes.

During the past 30 years electrical conductance measurements of aqueous electrolyte solutions, such as alkali chlorides and hydroxides [1-5], were carried out at ORNL utilizing a static high-pressure cell to conditions of 800°C and 400 MPa. The major disadvantages of this design are its limited accuracy at lower densities ($\rho < 0.4$ g·cm^{-3}), due to the high intrinsic conductance of the cell, and the inherently large temperature gradient along the vertical axis of the cell. These effects coupled with the high residence time of the solutions in the cell and auxiliary tubing, limited the concentration range that can be measured reliably to >0.001 mol·kg^{-1}. For weak electrolytes, accurate measurements need to be made at some much lower concentrations, especially at elevated temperatures. In 1995, Zimmerman *et al.* [6] built the first flow-through conductance cell functioning to the critical temperature of pure water. The cell operated with unprecedented accuracy for aqueous LiCl, NaCl, NaBr, and CsBr solutions at concentrations as low as 10^{-7} mol·kg^{-1}, at temperatures 306 - 400°C, and at pressures up to 28 MPa . However, this apparatus was not designed to operate at temperatures > 400°C and higher pressures. The new cell reported here was adapted from the existing static pressure vessel and will eventually serve to provide precise conductance measurements to 600°C and 300 MPa.

DESIGN AND OPERATION

The design and operation of the flow-through conductance cell are described in detail in another paper [7]. The configuration of the cell is shown schematically in Fig. 1, incorporating a coaxial electrode arrangement. The cell is suspended horizontally inside a ceramic tube furnace. The entire apparatus includes: heat and pressure generators, control and monitoring systems; a sample inlet delivery system with a 17- mL titanium-metal sample loop; and a Wayne Kerr electronic bridge.

Figs.2a, b and c present a cross-sectional view and dimensions of the tubular conductance cell, which consists of a Udimet high-pressure vessel [2] housing platinum (90%)-rhodium (10%) (Pt/Rh) alloy tubing, gold gaskets and the sapphire (rutile for LiOH) insulator. At each end of the vessel, the bore is enlarged to accommodate two stainless steel holders, which support the inlet and outlet Pt/Rh tubes and high pressure seals. The pressure seals consist of consecutive 20%-graphite-filled Teflon and Teflon packing. The input flow to the cell is routed through a series of Pt/Rh tubes gold-welded together and finally a Pt/Rh cup. The cup, which is in electrical contact with the Udimet vessel wall and serves as the outer electrode, is coated on the inside with platinum black. The inlet tubes are retained in position by three consecutive stainless steel (SS) tubes, which provide good thermal contact with the high-pressure vessel. The outflow from the cell is routed directly through a slit cut near the base of the inner electrode. The outer surface of the inner electrode is also coated with platinum black. Flow continues through another series of gold-welded Pt/Rh tubes. The inner electrode protrudes from an insulation disc (sapphire or rutile) and extends about one cm into the cup. One annealed gold washer is placed on the rim of the cup to create the seal between the sample chamber and the insulator. Another annealed gold washer, backed by Pt/Rh and SS discs, is located on the down-stream side of the insulator to provide support and a cushion for the insulator. The outflow Pt/Rh tubing passes through, and is electrically insulated by, a non-porous sintered alumina tube and a Teflon tube (starting from *ca.* 5 cm within the alumina tube and extending to the end of the outlet Pt/Rh tube). The Teflon-insulated Pt/Rh tube first passes through three pairs of Belleville springs, a SS retainer and a SS holder, then extends out of the Udimet vessel and into a low-temperature, high-pressure receiving vessel.

The high-pressure Udimet vessel is suspended horizontally within a tube furnace. The extreme ends of the vessel are cooled (from 25 up to 60°C) by copper coils through which water is circulated from an external thermostat in order to protect the 20%-graphite-filled Teflon sealing material and the Teflon insulating tube inside the furnace. The tube furnace is 30.48 cm long, 20.32 cm OD, and 4.128 cm ID with a total wound portion of Nichrome V (max. 1010°C) furnace wire of 22.86 cm. The windings are divided into three segments or heating zones. The 10.16 cm long middle zone of the furnace is the primary heat source for the cell body, whereas the two 6.35 cm long outer zones augment the middle zone by minimizing the temperature gradient along the cell. Furnace power and temperature control is provided by a CIMAC II process controller (Barber-Colman). At the center of the furnace is a SS sleeve (7.62 cm long) that fits snugly around the Udimet vessel and has a hole drilled to accommodate an Instrulab RTD, which provides an analog output that has been adapted as the main feedback control. The instrument has been calibrated to the ITS90 scale with a

digital resolution of ±0.01°C. The two outer zones of the furnace are controlled via standard K-type sheathed thermocouples, which are connected directly to the two remaining output devices. The performance of the system is such that stable temperatures are observed for long time periods with a maximum uncertainty in the reading of ±0.02°C at 400°C. Currently pressures up to 40 MPa are obtained by means of nitrogen gas supplied from a 40 MPa gas cylinder to the receiver pressure vessel and hence also into the void volume between the inner Pt/Rh tubing and the inner walls of the Udimet vessel. In the future, pressures above 40 MPa will be reached using an air-driven diaphragm pump in conjunction with a hydraulically-operated intensifier. Pressure is currently controlled by two back-pressure generators (Tescom) and monitored by strain-gauge transducers, which are connected to a dual channel digital readout gauge (Precise Sensors). The accuracy of the pressure measurements is ±0.1% of full scale. Pressure fluctuations controlled by the two back pressure regulators all about ± 0.1 MPa, resulting in resistance changes of about 0.4% at 300°C. The electrical resistance is measured with a Wayne Kerr 6425 Component Analyzer.

The experimental procedures are also described in detail in ref. 7. Deionized water contained in a glass reservoir heated to *ca.* 55 °C under a purge of argon is used as carrier solvent, whereas the solution is delivered to the sample loop by a commercial solvent delivery pump. Note that at pressures >5 MPa, the loaded sample loop is pre-pressurized to the equivalent pressure in the cell by means of a hand pump, thereby avoiding thermal shocks to the insulator (sapphire or rutile). The flow rate at temperatures ≤300°C is 0.05 mL·min^{-1} during measurements and 0.15 mL·min^{-1} at temperatures >300°C. For each sample series, the resistance of the solvent water was measured first before the measurement of sample solutions at frequencies from 0.5 to 10 kHz and extrapolated (resistance versus the reciprocal square root of frequency) to infinite frequency by a simple linear regression.

The concentrated stock solutions of NaCl (ultra pure, 99.999%, Baker) were prepared using conductivity water and stored in polyethylene bottles under argon and all weights of the stock solutions were corrected to vacuum conditions. The stock solutions of LiOH were prepared in the same manner as described in ref. 5. The conductivity water used in the preparation of the stock solutions was obtained by bubbling argon through distilled, deionized water for at least 30 minutes yielding a specific conductance of 1 to 4 x 10^{-7} Siemens·cm^{-1}. Dilute solutions were prepared by adding aliquots of the concentrated stock solution from polyethylene syringes to "confirmed," conductivity-grade water under agron, as mentioned previously. A series of sample solutions in the concentration range of 10^{-5} to 10^{-3} mol·kg^{-1} was prepared by consecutively adding stock solution to the most diluted sample solution.

The cell constant at 25°C is approximately 0.2 cm^{-1} as determined by measuring the resistance of 10^{-4} to 10^{-3} mol·kg^{-1} KCl solutions and calculated according to equations given by Justice [8], adjusted to the ITS90 scale. The exact value of cell constant is dependent upon the specific dimensions of the electrode assembly. Molality was converted to molarity using density data for KCl at 25°C calculated from the partial molar volumes of KCl at 25°C [9]. Cell constants obtained at 25°C from six to seven samples were in agreement to within ±0.2%. The cell was then heated to 400°C (30 MPa), and allowed to cool to 25°C, whereupon the cell constant was generally observed to change less than 0.3%. The cell constant is corrected for the thermal expansion of sapphire (or rutile) and platinum (less than 0.1% at 400°C).

RESULTS AND DISCUSSION

Preliminary measurements with this system were carried out to establish a reproducible and precise experimental method using available commercial pumps and tubing that are rated to 104 MPa. Therefore, studies of the conductivity of dilute aqueous NaCl and LiOH were made over a concentration range 10^{-5} to 10^{-3} mol·kg^{-1} at temperatures 250 - 405°C and 100 - 400°C, respectively, and pressures up to 32.5 MPa for comparison with reported results [5,6].

Fig.3 illustrates the percentage differences between experimental values (Λ_{expt}) of NaCl at 390°C and 32.5 MPa, and those (Λ_{calcd}) obtained by least-squares fit using the FHFP (Fuoss-Hsia-Fernández-Prini) equation [10] (eq. 1) as a function of the molar concentration for the solutions.

$$\Lambda = \alpha(\Lambda_0 - S(\alpha c)^{1/2} + E\alpha c \ln(\alpha c) - J_1\alpha c + J_2(\alpha c)^{3/2}) \quad (1)$$

where α is the degree of dissociation calculated from the mass action equation with the mean activity coefficient $\gamma_\pm$ of the free ions calculated based on the Debye-Hückel law,

$$K_A(M) = \rho K_A(m) = (1-\alpha)c/(\alpha^2 c\gamma_\pm^2) \quad (2)$$

$$\ln \gamma_\pm = -\kappa q\alpha^{1/2}/(1 + \kappa a\alpha^{1/2}) \quad (3)$$

and S, E, J_1, and J_2 in eq. 1 bear the same meaning and are calculated according to equations given in ref. 10, whereas in eqs. 2 and 3, $K_A(M)$ and $K_A(m)$ are the molar and molal association constants, respectively; ρ is the solvent density; κ is the reciprocal radius of the ionic atmosphere; q is the Bjerrum distance, a is the distance of the closest approach set equal to q according to the recommendation of Justice [8].

The deviations between $\Lambda_{expt.}$ and $\Lambda_{calcd.}$ using the best fit of each data set with eq.1 are generally less than 0.4%. The results show an improvement of greater than one order of magnitude in the precision of conductance measurements using the static cell and at least an order of magnitude in terms of the lowest solute concentration that can be measured [1-5]. The solution densities were computed from the partial molar volumes of NaCl [11-13], LiOH [14], NaOH [15] and using water densities [16] at the experimental temperatures and pressures. The values for Λ_0 of $LiOH_{(aq)}$ and $NaCl_{(aq)}$ as shown in Figs. 4 a and b are in good agreement with the reported values of NaCl [2,6,17-19] and LiOH [5, 20, 21] at corresponding conditions. Figs. 5a and b present the comparison of log $K_A(m)$ values with those reported for NaCl [2,6,17-19] and LiOH [5], respectively. They are in excellent agreement within the experimental uncertainties.

ACKNOWLEDGMENTS

This research project was sponsored by the Division of Chemical Sciences, Office of Basic Sciences and Engineering of the U.S. Department of Energy, under Contract DE-AC-05-96OR222464 with Oak Ridge National Laboratory managed by Lockheed Martin Energy Research Corporation, by International Association of the Properties of Water and Steam, and by the National Science foundation under Grant CHE 9725163.

REFERENCES

[1] A. S. Quist and W. L. Marshall, *J. Phys. Chem.*, Vol 72, 684-703, 1968.

[2] P. C. Ho, D. A. Palmer, and R. E. Mesmer, *J. Solution Chem.* Vol 23, 997-1018, 1994.

[3] P. C. Ho and D. A. Palmer, *J. Solution Chem.*, vol 25, 711-729, 1996.

[4] P. C. Ho and D. A. Palmer, *Geochim. Cosmochim. Acta* , vol 61, 3027-3040, 1997.

[5] P. C. Ho and D. A. Palmer, *J. Chem. Eng. Data*, vol 42, 162-170, 1998.

[6] G. H. Zimmerman, M. S. Gruszkiewicz, and R. H. Wood, *J. Phys. Chem.*, vol 99, 11612-11625, 1995.

[7] P. C. Ho, H. Bianchi, D. A. Palmer, and R. H. Wood (in preparation), 1999.

[8] J. C. Justice, *Compr. Treatise Electrochem., vol 5*, pp. 223-337, 1983.

[9] A. J. Ellis, *J. Chem. Soc. A*, 1579-1584 , 1966.

[10] R. Fernandez-Prini, *Physical Chemistry of Organic solvent Systems*, 1973, ch.5 pp. 525-614.

[11] D. F. Grant-Taylor, *J. Solution Chem.*, vol 10, 621-630, 1981.

[12] V. Majer, J. A. Gates, A. Inglese, and R. H. Wood, *J. Chem. Thermodynamics*, vol 20, 949-968, 1988.

[13] V. Majer and R. H. Wood, *J. Chem. Thermodynamics*, vol 26, 1143-1166, 1994.

[14] H. R. Corti, R. Fernandez Prini, and F. Svarc, *J. Solution Chem., vol* 24, 121-132, 1995.

[15] J. M. Simonson and R. J. Ryther, *J. Chem. & Eng. Data*, vol 34, 57-63, 1989.

[16] P. J. Hill, *J. Phys. Chem. Ref. Data* vol 19, 1233-1274, 1990.

[17] M. S. Gruszkiewicz and R. H. Wood, *J. Phys. Chem., vol* 101, 6549-6559, 1997.

[18] D. Pearson, C. S. Copeland, and S. W. Benson, *J. am. Chem. Soc., vol* 85, 1044-106, 1963.

[19] A. A. Noyes, *The Electrical conductivity of aqueous Solutions*, Carnegie Institute of Washington, publication, 1907, No. 63.

[20] H. R. Corti, R. Crovetto, and R. Fernandez-Prini, *J. Solution Chem., vol* 12, 897-908, 1979.

[21] J. M. Wright, W. T. Lindsay, and T. R. Druga, *The behavior of electrolytic solutions at elevated temperatures as derived from conductance measurements*, WAPD-TM-204, Westinghous, Tech. Service, Dept. Of Commerce, Washington, DC, 1961.

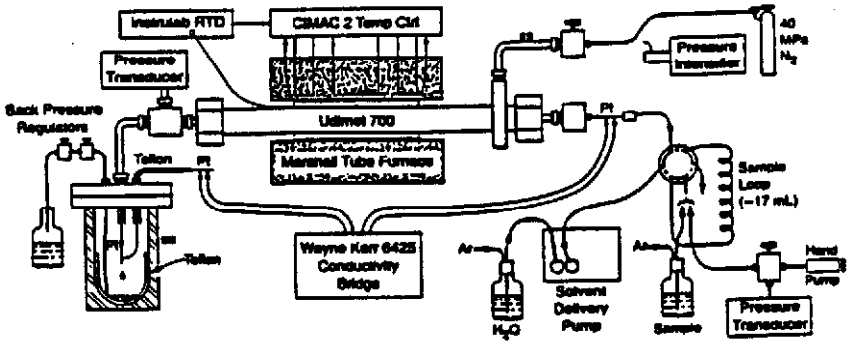

Fig. 1 Schematic diagram of the flow-through conductance measurement system.

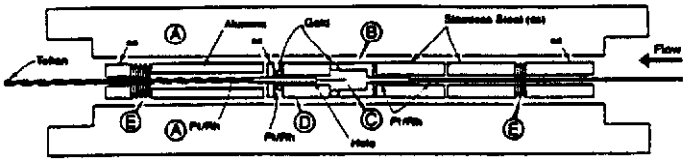

Fig. 2a Cross-sectional view of the tubular, flow-through conductance cell: (A) high-pressure vessel, (B) Pt/Rh cell chamber, (C) Pt/Rh inner electrode, (D) Sapphire or Rutile Insulator and (E) Belleville washer springs.

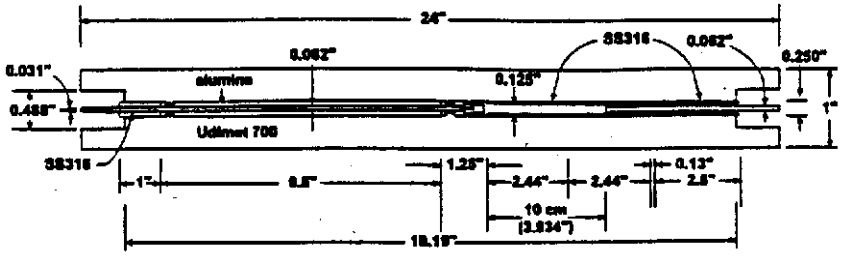

Fig. 2b Cross-sectional view and dimensions of the flow-through conductance cell.

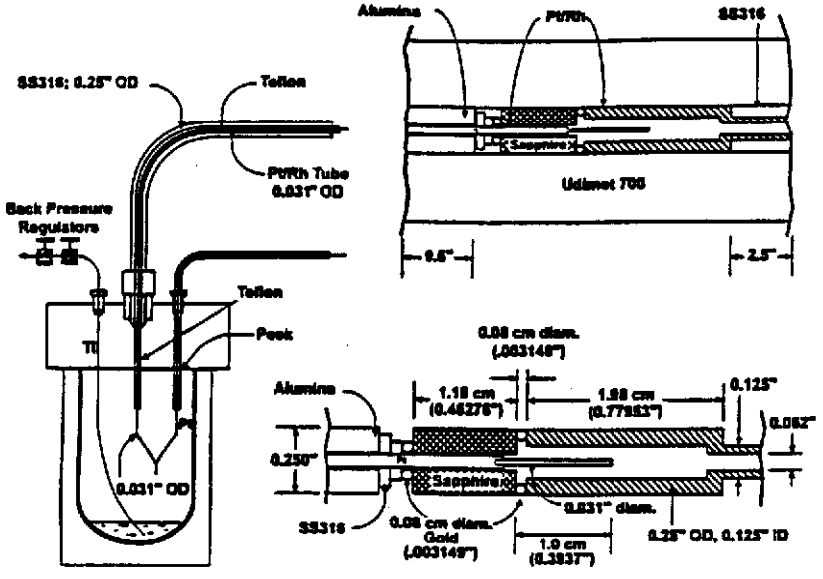

Fig. 2c Cross-sectional view and dimensions of the flow-through conductance cell.

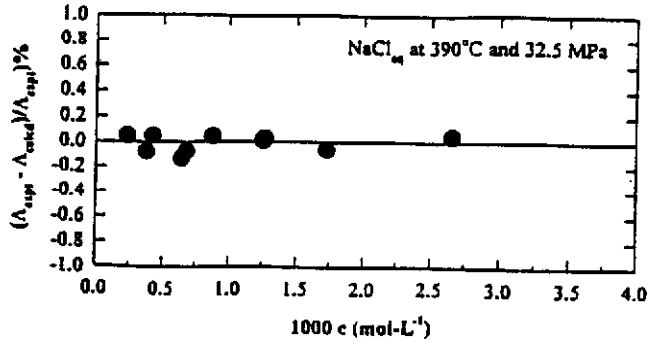

Fig. 3 Deviations of experimental and calculated values of Λ of NaCl at 390°C and 32.5 MPa as a function of molarity.

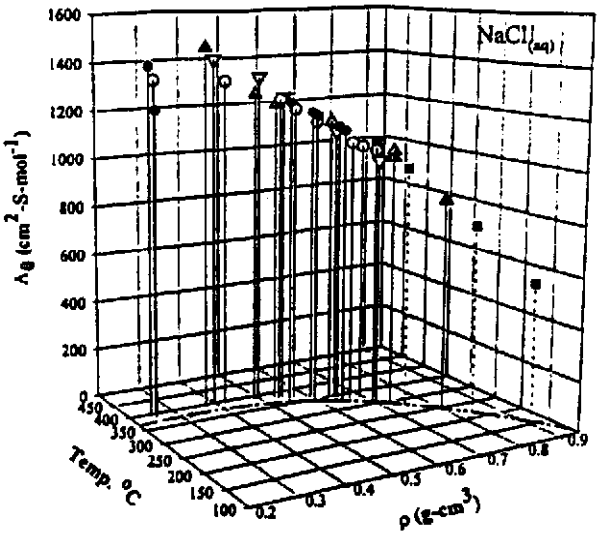

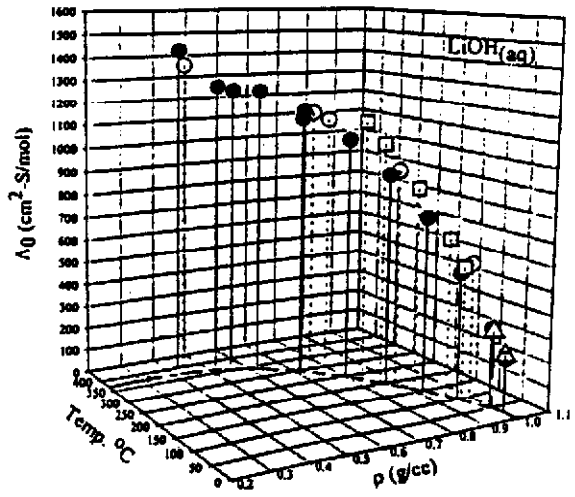

Fig. 4 Comparison of Λ_0 values of (a) for $NaCl_{aq}$: Ho *et al.* [2] (▽), this study (△), Zimmerman *et al.* [6] (○), Gruszkiewicz and Wood [17] (●), and Noyes [19] (■); and (b) for $LiOH_{aq}$: Ho and Palmer [5] (○). this study (●), Corti *et al.* [20] (△), and Wright *et al.* [21] (□) as functions of temperature and density at corresponding conditions.

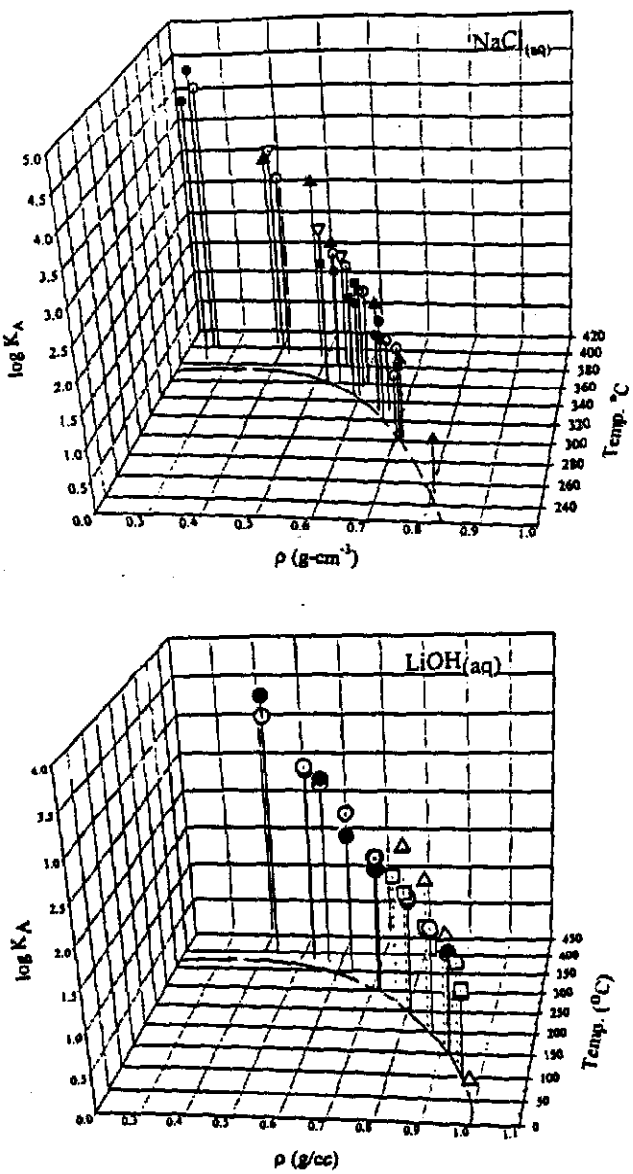

Fig. 5 Comparison of log K_A of (a) for $NaCl_{aq}$: Ho *et al.*[2] (▽), this study (△), Zimmerman *et al.* [6] (○), Gruszkiewicz and Wood [17] (●), and Pearson *et al.*,[18] (■); and (b) for $LiOH_{aq}$: Ho and Palmer [5] (○), this study (●), Corti *et al.* [20] (△), and Wright *et al.*[21] (□) as functions of temperature and density at corresponding conditions.